# Gut Pathogen Replication in the Absence of NINJ and Gasdermin-Mediated Plasma Membrane Rupture

By

Bingyue Zhou

BS, University of Toronto, 2024

Thesis

Submitted in partial fulfillment of the requirements for the Degree of Master of Science in the Graduate Program of Biotechnology at Brown University

PROVIDENCE, RHODE ISLAND

May 1st, 2026

AUTHORIZATION TO LEND AND REPRODUCE THE THESIS

**As the sole author of this thesis, I authorize Brown University to lend it to other institutions for the purpose of scholarly research.**

Date: May 1st, 2026 Bingyue Zhou

**I further authorize Brown University to reproduce this thesis by photocopying or other means, in total or in part, at the request of other institutions or individuals for the purpose of scholarly research.**

**Note: Chapter 1 of this thesis has been submitted to Journal of Alzheimer's Disease Reports and is under consideration for publication in 2024.**

Date: May 1st, 2026 Bingyue Zhou

This thesis by (Bingyue Zhou) is accepted in its present form by the Graduate Program in Biotechnology as satisfying the thesis requirements for the degree of Master of Science

Date_____ Signature: _____

Dr. Sanghyun Lee Advisor

Date_____ Signature: _____

Dr. Lalit Beura, Reader

Date_____ Signature: _____

Dr. Adam Crego, Reader

Approved by the Graduate Council

Date_____ Signature: _____

Dr. Thomas Lewis, Dean of the Graduate School

## Acknowledgments

I would like to express my heartfelt gratitude to the people who have supported me throughout this journey.

To my parents, thank you for your love, patience, and daily encouragement phone call. Your support has meant more to me than I can express with words. Through every challenge and moment of doubt, you have always stood by me. This accomplishment is as much yours as it is mine.

To my PI Sanghyun, I am deeply grateful for your guidance, leadership, and the knowledge you shared with me. Thank you for providing me with every opportunity to learn during my time in the lab, I will take the knowledge with me as far as I go. Your mentorship has played a meaningful role in shaping both this thesis and my development as a researcher.

To my lab mates, Li, Jaewon, Seokoh, Nola, Vashist, Yao, Christine, Joselynn, and Paul thank you for your support, kindness, and teamwork. Your help, encouragement, and shared understanding made this journey lighter and more rewarding. I truly appreciate the moments when you offered advice, solved problems with me, and created an environment where I could keep moving forward.

I would also like to thank my thesis panelists Dr. Beura and Adam for attending my defense and for the valuable insights and thoughtful feedback you provided. Your comments were truly appreciated and will help strengthen my work and future growth.

Finally, I want to thank myself for the determination, resilience, and hard work it took to reach this point. This journey challenged me in many ways, and I am proud of how far I have come. I have grown tremendously through this experience, and I believe I am ready for whatever comes next.

## Table of Contents

## Table of Tables and Figures

## Introduction

Cell death is fundamental for maintaining homeostasis in multicellular organisms. In response to environmental insults, infection, or DNA damage, cells activate signaling pathways that initiate death in a controlled and regulated manner, commonly referred to as programmed cell death. Programmed cell death occurs in three major modalities: apoptosis, necroptosis, and pyroptosis (Imre et al., 2020). Apoptosis is characterized by nuclear condensation, membrane blebbing, and subsequent phagocytic clearance by neighboring cells. In contrast, necroptosis and pyroptosis are more inflammatory and lytic forms of cell death (Nössing et al., 2023). These latter pathways are defined by early loss of plasma membrane integrity or plasma membrane rupture (PMR), leading to osmotic imbalance, membrane rupture, and the release of damage-associated molecular patterns (DAMPs) and pathogen-associated molecular patterns (PAMPs) (Shen et al., 2023). These molecules later lead to inflammation and activation of immune cells such as macrophages and neutrophils.

PMR represents the defining hallmark of lytic cell death and the irreversible point at which a cell can no longer maintain a biochemical boundary from the extracellular environment. This loss of membrane integrity is represented by the release of intracellular contents including DNA, inflammatory cytokines, and lactate dehydrogenase (LDH); alongside the passive uptake of membrane-impermeant dyes such as trypan blue and propidium iodide (Dondelinger et al., 2023). Despite recent advances in identifying the protein effectors that execute PMR, the precise molecular mechanisms within this process remain incompletely understood, making it an active and compelling area of investigation.

**Gasdermin D and Gasdermin E During Lytic Cell Death**

PMR was previously thought to result passively from osmotic pressure caused by cell swelling. This view was fundamentally challenged when two studies independently identified gasdermin (GSDM) family proteins as direct effectors responsible for driving PMR (Shi et al., 2015; Kayagaki et al., 2015). These proteins are activated by proteolytic cleavage by inflammatory caspases in response to cell death signals, making them key components of innate immunity, infectious disease, and cancer biology. Adding to their biological significance, evolutionary analyses have revealed that the GSDM family is highly conserved across species and represents an ancient protein family that emerged over 500 million years ago, highlighting its importance in maintaining cell metabolism (Angosto-Bazarra et al., 2022).

In terms of mechanism, Sborgi et al. demonstrated through a series of in vitro experiments that activated Gasdermin D (GSDMD) is sufficient to independently form β-barrel pores in lipid membranes, establishing it as a direct effector of pyroptosis (Sborgi et al., 2016). Gasdermin E (GSDME) was subsequently shown to promote lytic cell death through a comparable pore-forming style, though its role was initially uncovered in a distinct context: chemotherapy-induced activation of caspase-3 was found to cleave and activate GSDME (Wang et al., 2017) (Figure 1).

Though the discovery of GSDM pore-forming activity offered a compelling framework for PMR, it did not capture the full picture. GSDM pores are constrained in diameter and are insufficient to permit the passage of bulkier molecules such as lactate dehydrogenase (LDH), leaving a critical gap in the understanding of how terminal plasma membrane rupture is achieved (Evavold et al., 2018; Borges et al., 2022). This gap was subsequently addressed by the

identification of a distinct class of membrane proteins, ninjurin proteins (NINJ), as downstream mediators of large-scale membrane disruption (Kayagaki et al., 2021).

**NINJ1 and NINJ2 During Lytic Cell Death**

A forward genetic screen conducted around the year of 2021 identified NINJ1 as another critical mediator of PMR. Human NINJ1 is a 16 kDa protein consisting of 152 residues that is evolutionarily conserved across many higher eukaryotes (Degen et al., 2023). It is widely expressed in cells with epithelial origin, including gut epithelial cells (Araki and Milbrandt, 1996). Structurally, the first 38 amino acids constitute a non-structural region that is confirmed to be dispensable for function according to deletion experiments (Degen et al., 2023). Residues 39–141, by contrast, were modelled unambiguously as four α-helices (α1–α4) based on AlphaFold predictions and NMR data (Degen et al., 2023). Among the helices, α-3 and α-4 are transmembrane domains that can be embedded in the plasma membrane, α-1 and α-2 are extracellular domains (Figure 1). Macrophages lacking NINJ1 exhibit markedly impaired membrane rupture and fail to release pyroptotic markers such as LDH (Kayagaki et al., 2021).

Mechanistically, activated NINJ1 first forms dimers and trimers, which subsequently polymerize into larger molecular structures through side-chain interactions between helices of adjacent NINJ1 molecules (Figure 1). They eventually assemble in a fence-like arrangement along the plasma membrane (Degen et al., 2023). These polymeric assemblies drive membrane fragmentation through the formation of membrane disks that are shed into the extracellular space, ultimately releasing intracellular contents and completing lytic cell death (Degen et al., 2023; David et al., 2024). Given the high degree of conservation between human and murine

NINJ1, the mechanistic framework described above is expected to apply to the mouse models used in this study.

NINJ2 is a close paralog of NINJ1, consisting of 143 residues and sharing homologous transmembrane helices, but lacking a comparable N-terminal adhesion motif (Araki and Milbrandt, 1999). In terms of expression, NINJ2 is most abundant in immune organs and bone marrow, with moderate expression in the gut epithelium, suggesting a potentially relevant but understudied role in intestinal biology (Araki and Milbrandt, 1999). Despite its structural similarity to NINJ1, recent cryo-EM studies have shown that NINJ2 is incapable of oligomerization, as the curvature of the NINJ2 filament is physically incompatible with membrane solubilization or pore formation. These structural findings led researchers to conclude that, unlike NINJ1, NINJ2 does not mediate plasma membrane rupture (Sahoo et al., 2025).

Despite lacking a direct role in PMR, emerging evidence suggests that NINJ2 participates in other aspects of homeostasis. Loss of NINJ2 has been shown to sensitize cells to ferroptosis, an effect linked to impaired lysosomal homeostasis (Zhang et al., 2026). Separately, Ninj2-deficient mice have been reported to experience shortened lifespan and spontaneous tumor formation, with loss of NINJ2 promoting pyroptosis through activation of the NLRP3 inflammasome (Zhang et al., 2024). Together, these findings highlight that although NINJ2 is structurally incapable of directly mediating PMR, it appears to play a modulatory role in cell death regulation through at least two independent mechanisms — inflammasome-driven pyroptosis and iron-dependent ferroptosis.

Although NINJ and GSDM family members were identified through independent discoveries, emerging evidence suggests that they operate in a coordinated manner during lytic

cell death. NINJ1 oligomerization has been shown to coincide temporally with gasdermin activation, as NINJ1 polymers are found to coexist with cleaved GSDMD p30 at the plasma membrane during pyroptosis, indicating that NINJ1-mediated membrane rupture occurs alongside rather than downstream of GSDMD pore formation (Degen et al., 2023). This temporal overlap suggests that PMR is not driven by a single effector acting in isolation, but rather emerges from the coordinated action of multiple membrane-disrupting proteins. Together, the discoveries of GSDMD, GSDME, and NINJ1/2 have fundamentally redefined plasma membrane rupture as an active and regulated cellular process, rather than a passive consequence of osmotic imbalance, and raise important questions about how this multi-effector system operates in the context of infection in vivo.

**Host-pathogen Interactions and Ninjurin proteins**

Given the established role of NINJ1 in mediating plasma membrane rupture, its involvement in host–pathogen interactions is not unexpected. Emerging evidence suggests that NINJ1 contributes to host defense during infection. $NINJ1^{-/-}$ mice show increased susceptibility to infection with *Citrobacter rodentium* compared to wild-type controls, as demonstrated by reduced survival rates in knockout animals (Kayagaki et al., 2021). Consistent with these findings, another study reported that $Ninj1^{-/-}$ macrophages are more susceptible to herpes simplex virus type 1 (HSV-1) infection than wild-type cells (Hartenian et al., 2026). Together, these studies support a protective role for NINJ1 in certain infectious contexts.

However, more recent work by Song et al. revealed a distinct and context-dependent role for NINJ1 during murine norovirus (MNoV) infection. In this model, NINJ1 is co-opted by the

virus to facilitate infection in the gut. Specifically, NINJ1 directly interacts with the viral protein NS1 and promotes plasma membrane rupture, enabling NS1 release (Song et al., 2025). In NINJ1 knockout (KO) cells, NS1 secretion is markedly impaired (Song et al., 2025). Previous work from the same group demonstrated that NS1 protein from MNoV can effectively suppress inflammatory cytokine responses (Lee et al., 2019). Therefore, NINJ1$^{-/-}$ cells in this case may contribute to lower susceptibility to MNoV and potentially a less severe phenotype. These findings contrast with the protective effects observed in bacterial and HSV-1 infection models, highlighting the fact that NINJ1's role in infection is highly dependent on the context. Depending on the pathogen and target tissue, NINJ1 may either promote host defense or be exploited by viruses to enhance pathogenesis.

**Gut Infection and PMR Effector Screening**

With the understanding of the context-dependent roles of PMR effectors in infection, an important question arises: how does the absence of key membrane-disrupting proteins such as GSDMD, GSDME, and NINJ1 influence infection in vivo? Much of the current evidence has been derived from two-dimensional cell culture systems or isolated primary mouse cells, which do not fully capture the complexity of host–pathogen interactions within an intact organism.

To address this gap, this thesis examined enteric viral infections in genetically modified mice lacking specific PMR effectors. Knockout and wild-type mice were infected with gut-associated viruses—including rotavirus, murine astrovirus, and murine norovirus—to determine whether PMR pathways influence viral replication and infection dynamics in vivo.

Rotaviruses are double-stranded RNA viruses that infect the gastrointestinal epithelium and represent one of the leading causes of acute gastroenteritis (AGE) in children under five

years of age (Pawłuszkiewicz et al., 2025). Rotavirus pathogenesis is characterized by loss of microvilli, mitochondrial swelling, and expansion of the endoplasmic reticulum. These pathological features have been linked to activation of cell death pathways, including apoptosis (Pawłuszkiewicz et al., 2025). Given the involvement of epithelial damage and cell death during infection, it is important to investigate whether PMR processes contribute to rotavirus pathogenesis.

Murine astrovirus is a single-stranded RNA virus that is highly prevalent in laboratory mice (Ingle et al., 2021). It is frequently used as a model to study astrovirus biology, as human astrovirus lacks robust small animal models. Astrovirus infection of the gut is generally associated with minimal inflammation and limited epithelial damage; however, extra-intestinal manifestations, including encephalitis and meningitis, have also been reported (Morita et al., 2021). These features raise questions about how host cell death pathways may influence viral persistence and tissue tropism.

Murine norovirus, another enteric RNA virus, is estimated to cause approximately 20 million cases of gastroenteritis annually in humans (Hall et al., 2016). As discussed above, noroviruses can exploit non-structural proteins such as NS1 to modulate host immune responses and enhance viral replication in enterocytes (Lee et al., 2019). The regulated release of NS1 makes norovirus particularly relevant for investigating potential interactions between viral egress mechanisms and plasma membrane rupture pathways.

By employing whole-animal models, this study provides a comprehensive assessment of how PMR effectors such as GSDMD, GSDME, NINJ1, and NINJ2 contribute to enteric viral infection.

## Results

### Generation of Mouse Models to study PMR effectors

To investigate the in vivo role of PMR effectors during enteric viral infection, a panel of genetically modified mouse models that lack key mediators of lytic cell death was generated. Given the context-dependent roles of these proteins reported in prior studies, we were particularly interested in whether these findings would be consistent or diverge in an intact organism. To capture both tissue and systemic contributions of PMR effectors, the panel included intestinal epithelium-specific conditional knockouts of *Ninj1, Ninj2,* and a combined *Ninj1 Ninj2* double knockout, all generated using the Cre-loxP system under the *Villin1* promoter (*Vil1*-Cre); as well as whole-body knockout lines for both *Ninj1* and *Ninj2*. A *GsdmD* and *GsdmE* double knockout (DKO) line was also included to assess the contribution from the gasdermin side. The mouse strains used in this study are summarized in Table 1.

For the *Ninj1* conditional allele, loxP sites were inserted flanking exon 2 using CRISPR-Cas9 with a sequence-specific sgRNA. Exon 2 spans approximately 229 base pairs (bp) and is shared across all annotated *Ninj1* transcripts, making it an ideal target for disrupting expression (Ensembl; Figure 2A). The floxed region encompassed approximately 1,390 bp of genomic sequence, including exon 2 and portions of the intronic sequences. Mice carrying the floxed allele were crossed with *Vil1*-Cre transgenic mice, in which Cre recombinase expression is driven specifically in intestinal epithelial cells, thereby restricting the deletion in a tissue-specific manner (Figure 2A). Upon Cre-mediated recombination, the floxed exon 2 is excised, producing a deletion allele in which the Ninj1 transcript splices directly from exon 1 to exon 3, introducing a frameshift and a predicted premature stop codon that abolishes functional NINJ1 protein expression (Figure 2A). Figure 2B illustrates a similar *Ninj1* knockout strategy, in

which exon 2 is flanked by loxP sites, but Cre recombinase expression is instead driven by the *ROSA26* promoter under the control of a tamoxifen-inducible CreERT2 system. Without tamoxifen, the CreERT2 protein is sequestered and remains inactive, leaving the floxed allele intact. However, with tamoxifen administration, the ERT2 domain binds and undergoes a conformational change that releases CreERT2, allowing it to perform recombination at the loxP sites. This results in whole-body excision of *Ninj1* exon 2 in all cell types that express ROSA26, generating a systemic Ninj1 knockout in adult mice (Figure 2B).

The strategy for generating *Ninj2* knockout models follows a broadly analogous approach to that of *Ninj1*. Exon 2 of *Ninj2* spans approximately 232 bp and is shared across all annotated Ninj2 transcripts (Ensembl). The loxP sites were positioned to flank a genomic region of approximately 1,245 bp, encompassing exon 2 along with portions of the surrounding intronic sequences (Figure 2C). As with *Ninj1*, gut-specific *Ninj2* knockout mice were generated by crossing the floxed allele with *Vil1*-Cre transgenic mice. For the whole-body conventional knockout, a distinct approach was employed where SpCas9 protein and an sgRNA were introduced directly into mouse embryos via microinjection at the one-cell stage, targeting a 1,152 bp genomic region encompassing exon 2 (Figure 2D). Founder mice derived from these gene-edited embryos were subsequently backcrossed to establish a stable germline transmission of the deletion allele, yielding a whole-body ubiquitous *Ninj2* knockout line. Deletion of exon 2 in both models results in a *Ninj2* transcript that splices directly from exon 1 to exon 3, introducing a frameshift and a predicted premature stop codon that abolishes functional NINJ2 protein expression. Analogous conditional knockout strategies were employed to generate gut-specific *Ninj1 Ninj2* double knockout mice, with both *Ninj1* and *Ninj2* exon 2 deleted (not shown in figure).

To further illustrate the rationale for targeting exon 2, the predicted amino acid sequences of NINJ1 and NINJ2 were examined. In NINJ1, exon 2 encodes the N-terminal adhesion motif and both transmembrane α-helices, which are the structural domains responsible for membrane anchoring and oligomerization that eventually drive PMR (UniProt). Its deletion therefore results in complete loss of these functional domains, rendering the knockout highly effective. Although NINJ2 domains are less well characterized, a comparable outcome is anticipated since its exon 2 similarly spans the two transmembrane α-helices. The exon 2-targeted Ninj knockout deletion is predicted to abolish membrane disruption.

Correct targeting was confirmed by PCR-based genotyping using allele-specific primer sets designed to distinguish the wildtype, floxed, and excised alleles. Later, qPCR was conducted using collected mice tissue for NINJ1 and NINJ2 mRNA expression levels (Figure 7). Following confirmation, mice were bred to homozygosity and subsequently used for infection experiments. Importantly, wildtype controls for the conditional knockout lines were not naive wildtype animals, but rather Cre-negative littermates carrying the floxed allele without the Cre recombinase transgene. This design ensures that any observed differences between groups reflect the consequence of gene deletion specifically, rather than potential confounding effects.

To assess the impact of PMR effector loss on enteric viral infection, adult mice from each genotype were infected with one of three gut-tropic RNA viruses: rotavirus, murine astrovirus (MAstV), or murine norovirus (MNoV) (Figure 3). For rotavirus infections, mice were inoculated by oral gavage with $10^5$ virions in 100 µl, and fecal pellets were collected at 2 and 4 dpi (Figure 3). For MAstV infections, mice received a previously titrated EV50 dose delivered by oral gavage via a P200 pipette in a volume of 25 µl, with fecal pellets and tissues harvested at 3 dpi. For MNoV infections, mice were inoculated with $10^6$ or $10^7$ plaque-forming units (PFU) of

the CR6 strain by oral gavage, and samples were collected at 3, 7, 14, and 21 dpi. For all infections, viral burden in the stool was quantified by qRT-PCR and expressed as genome copies per fecal pellet (Figure 3).

**Rotavirus Replication Is Unaffected by Loss of PMR Effectors**

To determine whether PMR effectors influence rotavirus infection dynamics in vivo, we quantified fecal viral RNA loads at 2 and 4 dpi across six genotypes: *Ninj1*$^{fl/fl}$ Vil1-Cre, *Ninj2*$^{fl/fl}$ *Vil1*-Cre, *Ninj1*$^{fl/fl}$ *Ninj2*$^{fl/fl}$ *Vil1*-Cre, *Ninj1*$^{fl/fl}$ *Rosa26*-CreERT2, *Ninj2-/-* , and *GsdmD-/- GsdmE-/-*. Rotavirus RNA was detectable in all animals at both timepoints, with all samples exceeding the limit of detection (LOD; $10^3$ genome copies per fecal pellet). Viral loads were distributed in the range of $10^4$–$10^7$ copies per fecal pellet and were broadly comparable between KO and WT animals within each genotype group (Figure 4).

No statistically significant differences in fecal rotavirus shedding were observed between KO and WT animals in any of the six genotypes at either timepoint (Mann–Whitney test, $p > 0.05$ for all comparisons). This was consistent across gut-epithelium-specific deletions via *Vil1*-Cre, tamoxifen-inducible systemic deletion via CreERT2, conventional *Ninj2* knockout, and combined gasdermin deficiency. Notably, even simultaneous intestinal ablation of both *Ninj1* and *Ninj2* did not produce a detectable change in viral burden at either timepoint, arguing against functional redundancy between the two paralogs as an explanation for the null result. These data indicate that NINJ1, NINJ2, GSDMD, and GSDME expressions are dispensable for productive rotavirus infection of the murine gut in vivo.

Some variability in WT baseline viral loads was observed across cohorts, particularly at 2 dpi. This inter-cohort variation likely reflects biological variability across independent infection experiments and was not associated with any consistent directional shift between genotypes.

**Astrovirus Shedding Is Not Significantly Altered by PMR Effector Deficiency**

We next assessed whether PMR effector loss affects murine astrovirus replication in the intestine. Fecal viral RNA was quantified at 3 dpi in three genotypes with complete datasets: *Ninj1*$^{fl/fl}$ Vil1-Cre, *Ninj2*$^{fl/fl}$ *Vil1*-Cre, and *GsdmD-/- GsdmE-/-*. Astrovirus genome copies were readily detectable in all animals, with viral loads clustering in the range of $10^6$–$10^8$ copies per fecal pellet (Figure 5).

No statistically significant differences in astrovirus shedding were detected between KO and WT mice in any of these three genotypes (Mann–Whitney test, $p > 0.05$ for all comparisons). These findings are consistent with the rotavirus data and suggest that gut-epithelial loss of NINJ1 or NINJ2, or whole-body loss of gasdermin effectors, does not meaningfully alter the replication or fecal shedding of murine astrovirus at 3 dpi.

**Murine Norovirus Replication Is Independent of NINJ1 and NINJ2 Status In Vivo**

We next assessed whether PMR effector loss affects murine norovirus replication in the gut. Fecal viral RNA was quantified at 3, 7, 14, and 21 dpi across three genotypes with complete datasets: *Ninj1*$^{fl/fl}$ *Vil1*-CreERT2, *Ninj1*$^{fl/fl}$ *ROSA26*-CreERT2, *Ninj2-/-* (Figure 6). MNoV genome copies were readily detectable in all animals at all timepoints, with viral loads consistently clustering in the range of $10^4$–$10^6$ copies per fecal pellet (Figure 6).

No statistically significant differences in fecal MNoV shedding were observed between KO and WT animals in any of the genotypes tested at any timepoint (Mann–Whitney test, $p > 0.05$ for all comparisons). Viral loads remained stable across the 21-day infection course in both KO and WT animals, suggesting that loss of Ninj1 or Ninj2, whether restricted to the intestinal epithelium or throughout the whole body, does not affect the establishment, magnitude, or persistence of MNoV infection in vivo. These findings are consistent with the rotavirus and astrovirus data, further supporting the conclusion that PMR effectors of the ninjurin family are dispensable for enteric viral infection under the conditions examined.

## Discussion

Taken together, these findings demonstrate that genetic ablation of NINJ1, NINJ2, GSDMD, or GSDME, individually or in combination and whether restricted to the intestinal epithelium or throughout the whole body, does not produce a statistically significant change in the replication or fecal shedding of rotavirus, astrovirus, or murine norovirus in vivo. These results suggest that PMR effectors of the NINJ and gasdermin families are dispensable for the course of these enteric viral infections under the conditions examined, and that the gut epithelium retains its capacity to support viral replication in the absence of these proteins.

These results invite consideration alongside existing literature. For instance, previous work has demonstrated that during murine norovirus infection, NINJ1 can be co-opted by the virus to facilitate the selective secretion of the viral protein NS1, a process important for establishing infection in the gut (Song et al., 2025). Similarly, rotavirus infection is known to induce cell death and epithelial damage through the activation of inflammasomes, pathways with which GSDMD oligomerization is associated (Dickson, 2017). The lack of a clear phenotype in our experimental mouse models was therefore somewhat unexpected.

Several factors may account for the differences between our observations and those reported in cell culture or ex vivo systems. First, it is possible that the experimental timepoints chosen for viral load measurement did not capture the peak of any potential effect. For example, while norovirus NS1 secretion occurs during infection, its impact on overall viral replication kinetics might be subtle or occur within a narrow window that was not resolved in our fecal shedding analysis.

Second, the redundancy and compensatory mechanisms within the cell death machinery may be more pronounced in vivo. The concurrent presence of multiple, functionally overlapping

pathways for membrane permeabilization could allow the intestinal epithelium to maintain its capacity to support viral replication even in the absence of key individual effectors like NINJ1 or gasdermins. Whether plasma membrane rupture itself was successfully blocked in the relevant cells during infection remains unknown. Future studies could address this by directly confirming PMR status. For example, transmission electron microscopy could be used to visualize membrane integrity. Alternatively, membrane-impermeant dyes could help quantify cell death in tissue sections. Such evidence would clarify whether the lack of a viral phenotype reflects true functional compensation or simply indicates that the genetic deletions did not fully eliminate PMR in the intestinal epithelium.

Additionally, the possibility of technical or experimental variability should not be ruled out. In particular, murine astrovirus is known to be highly prevalent in laboratory mouse colonies, and the facility housing the animals used in this study does not maintain active surveillance against this virus. It is therefore possible that some animals had been pre-exposed to MAstV prior to experimental infection. Such prior exposure could have generated protective immunity, potentially obscuring any effect of PMR effector loss on viral replication. This consideration underscores the importance of confirming pathogen status in future studies to ensure that baseline immune conditions do not confound experimental outcomes.

Furthermore, the inherent complexity of the in vivo intestinal environment, including contributions from the microbiota, immune cells, and the three-dimensional tissue architecture, may modulate the requirement for these specific PMR proteins in ways that cannot be fully recapitulated in simplified cell culture models. The lack of a phenotype could also suggest that these PMR effectors, while important for certain aspects of cell death and inflammation, are not critical for the basic replication cycle of these viruses within the gut of an organism.

Finally, it warrants consideration that the confirmation of successful functional knockout of these PMR effectors in the relevant intestinal cell types during active infection was not directly assessed in this study. It remains a possibility that residual protein function or compensatory upregulation of related proteins occurred in the knockout animals, which could have masked a potential phenotype.

In conclusion, while our findings do not align with some of the more pronounced effects seen in other systems, they highlight the complexity of host-pathogen interactions in-vivo. Further investigation will be required to determine whether these PMR pathways play more context-specific roles, such as in modulating the host inflammatory response rather than directly impacting viral replication, or whether their importance becomes apparent only under conditions of stress or co-infection.

Although the results of this study were not entirely as expected, they still offer meaningful insight into host-virus interactions. Much of the existing research in this area has focused on inflammation and immune-mediated defenses. By contrast, this study examined enteric viral infection from the perspective of cell death machinery, specifically plasma membrane rupture effectors. This alternative viewpoint helps broaden the understanding of how viruses and hosts interact at a fundamental cellular level. Inconsistencies such as these are not uncommon in a young and rapidly evolving field. They suggest that the roles of cell death pathways in infection are likely more nuanced than currently appreciated. By documenting these observations, this study contributes to a growing body of work that will ultimately help clarify how membrane rupture machinery influences viral pathogenesis.

## Methods and Materials

### Mouse Lines

C57BL/6J wildtype mice (strain #000664) and *GsdmD*$^{-/-}$ *GsdmE*$^{-/-}$ double knockout mice (C57BL/6N-*Gsdmd*em4Fcw/J, strain #032410; strain #032411) were obtained from the Jackson Laboratory. *Vil1*-Cre (strain #021504), *Vil1*-CreERT2 (strain #020282), and *Rosa26*-CreERT2 (strain #008463) transgenic Cre driver lines were also obtained from the Jackson Laboratory.

Conditional floxed alleles for *Ninj1* and *Ninj2* were generated in-house using CRISPR-Cas9. For *Ninj1*, loxP sites were inserted flanking exon 2 (~229 bp, shared across all annotated transcripts), encompassing approximately 1,390 bp of genomic sequence. For *Ninj2*, loxP sites were inserted flanking a ~1,245 bp region encompassing exon 2 (~232 bp, shared across all annotated transcripts). In both cases, Cre-mediated excision of exon 2 produces a transcript that splices directly from exon 1 to exon 3, introducing a frameshift and predicted premature stop codon that abolishes functional protein expression.

To generate gut-specific conditional knockout lines, *Ninj1*$^{fl/fl}$ and *Ninj2*$^{fl/fl}$ mice were independently crossed with *Vil1*-Cre transgenic mice, restricting exon 2 excision to intestinal epithelial cells. The intestinal *Ninj1*$^{fl/fl}$ *Ninj2*$^{fl/fl}$ *Vil1*-Cre double conditional knockout was generated by intercrossing the two floxed lines followed by crossing with *Vil1*-Cre mice. For the gut-specific inducible line, *Ninj1*$^{fl/fl}$ mice were crossed with *Vil1*-CreERT2 mice. For the systemic inducible knockout, *Ninj1*$^{fl/fl}$ mice were crossed with *Rosa26*-CreERT2 mice, in which tamoxifen administration induces whole-body excision of *Ninj1* exon 2 in adult mice. The conventional whole-body *Ninj2* knockout (*Ninj2*$^{-/-}$) was generated by direct microinjection of SpCas9 and sgRNA into mice embryos, targeting a 1,152 bp region encompassing exon 2. Founder mice

were subsequently backcrossed to establish stable germline transmission of the deletion allele. For all conditional knockout experiments, Cre-negative littermates, confirmed through genomic PCR, that carry the floxed allele were used as wildtype controls to the Cre-positive KO mice.

All mice were bred and housed at the Brown University facilities under specific pathogen–free conditions with food and water ad libitum and 12-hour day-night cycle. The mice used were sex and age matched. Male and female mice were used at 8 to 12 weeks of age. All animal experiments were approved by Brown University Institutional Animal Care and Use Committee (protocol #23-04-0002).

**Infection**

For MNoV infection, adult mice at 8 to 12 weeks of age were inoculated with $10^6$ or $10^7$ plaque-forming units of CR6 strain by the oral route in a volume of 25 µl. Fecal pellets and tissues were harvested into 2-ml tubes (Sarstedt) with 1-mm-diameter zirconia/silica beads (Biospec). Stool, colon, MLN, and ileum were harvested from these mice at 3, 7, 14, and 21 days post infection. Later these samples were flash frozen on dry ice and stored at −80°C until analysis.

For Rotavirus infection, adult mice at 8 to 12 weeks of age were treated with 1.33% $NaHCO_3$ dissolved in water. The mice were then left for 5-10 minutes, followed by inoculation with $10^5$ virions through the oral route in a volume of 100 µl. Fecal pellets were harvested into 2-ml tubes (Sarstedt) with 1-mm-diameter zirconia/silica beads (Biospec) at 2 and 4 days post infection. Mice were then sacrificed at 4 days post infection and tissue samples from the ileum, MLN, colon and spleen were collected. The samples were flash frozen by dry ice and stored at −80°C until analysis.

For Astrovirus infection, adult mice at 8 to 12 weeks of age were inoculated with a previously defined EV50 by the oral route in a volume of 25 μl. Fecal pellets and tissues were harvested at 3 days post infection into 2-ml tubes (Sarstedt) with 1-mm-diameter zirconia/silica beads (Biospec). Stool, duodenum, ileum, and colon were collected. The samples were flash frozen by dry ice and stored at −80°C until analysis.

**Statistical analysis**

Statistical analyses were performed using GraphPad Prism 10. All experiments were analyzed by two-tailed unpaired Mann–Whitney test with the Holm–Šídák correction for multiple comparisons. A p value of less than 0.05 was considered statistically significant.

## Figures

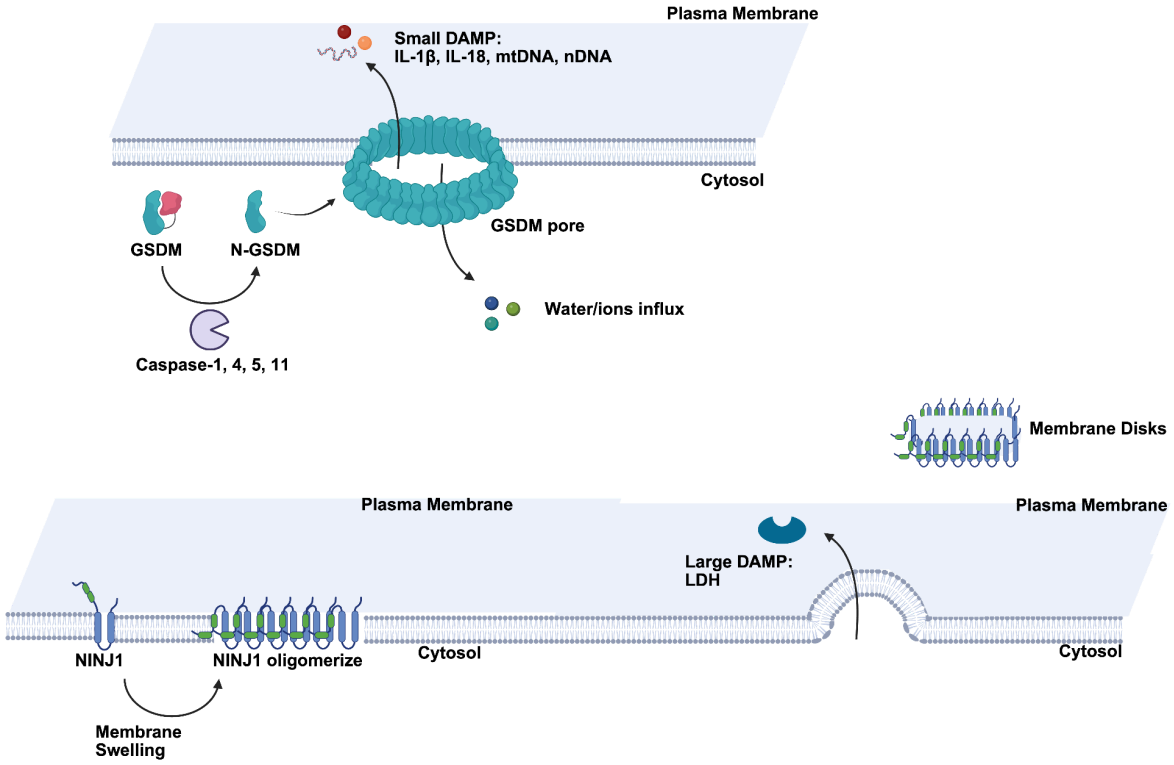


**Figure 1. Mechanisms of plasma membrane rupture mediated by gasdermin and NINJ1 during lytic cell death.**

**(Top)** Gasdermin (GSDM), upon cleavage by inflammatory caspases, oligomerizes to form large transmembrane pores in the plasma membrane. These pores are sufficient to permit the release of small damage-associated molecular patterns (DAMPs) including IL-1β, IL-18, mitochondrial DNA (mtDNA), and nuclear DNA (nDNA). However, the restricted diameter of GSDMD pores limits the passage of larger cytoplasmic contents. **(Bottom)** NINJ1 monomers, activated while sensing membrane swelling, oligomerize and polymerize to form membrane disks. These structures drive the shedding of membrane disks into the extracellular space, enabling the release of large DAMPs such as LDH. Together, GSDM-mediated pore formation and NINJ1-mediated membrane rupture represent two mechanisms in the execution of terminal lytic cell death. Adapted from Wang et al., 2025, *Journal of Biological Chemistry*, with permission from Elsevier.

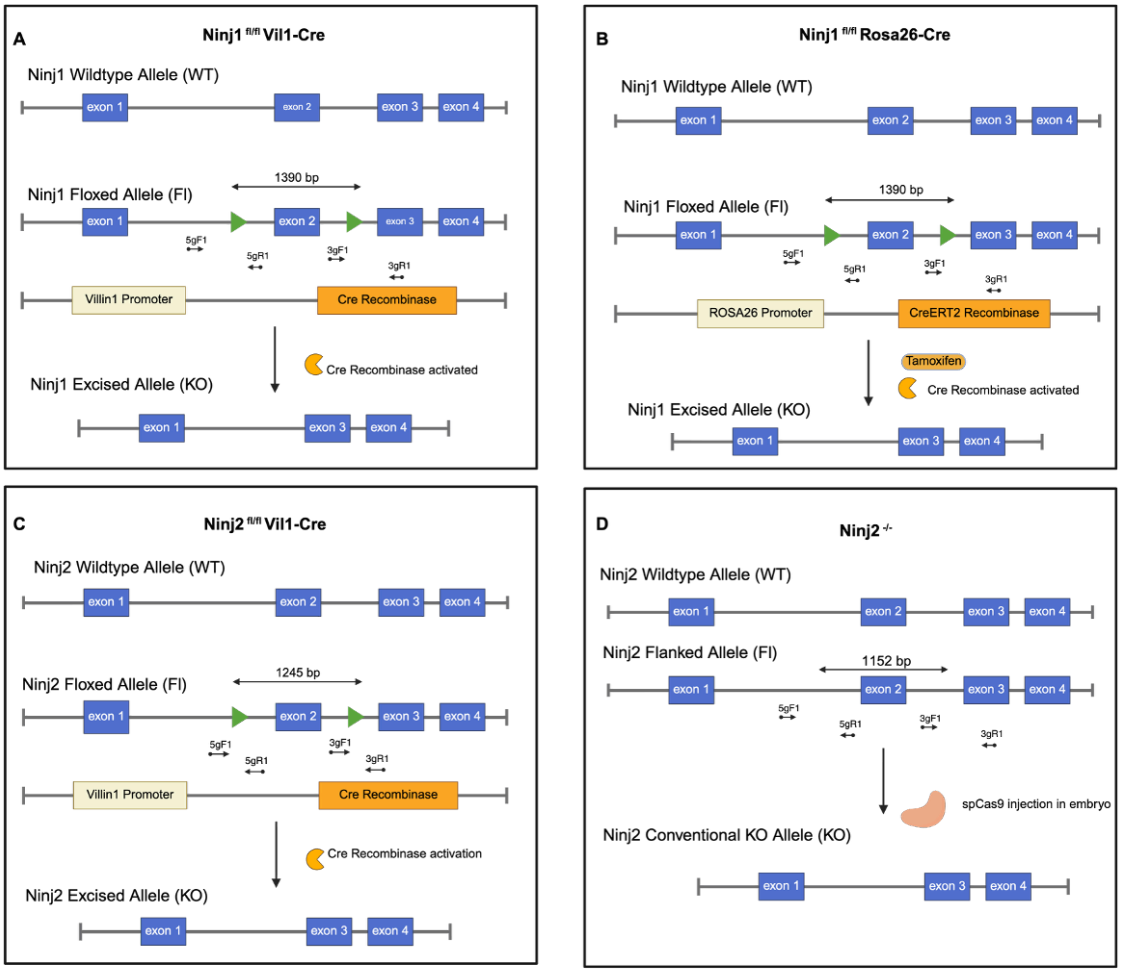


**Figure 2. Targeted gene disruption strategy for plasma membrane rupture effectors.** In all panels, the wildtype allele (top) and floxed allele (middle) show loxP sites (green triangles) flanking exon 2, with genotyping primer positions indicated by arrows. **(A)** Gut-specific *Ninj1* conditional knockout generated by crossing the floxed *Ninj1* allele with *Vil1*-Cre transgenic mice, restricting exon 2 excision to intestinal epithelial cells. **(B)** Tamoxifen-inducible whole-body *Ninj1* conditional knockout generated by crossing the floxed *Ninj1* allele with *Rosa26*-CreERT2 mice, in which Cre-mediated excision is activated upon tamoxifen administration. **(C)** Gut-specific *Ninj2* conditional knockout generated using the same *Vil1*-Cre strategy as in panel A. **(D)** Conventional whole-body *Ninj2* knockout generated by embryonic microinjection of SpCas9 and a sequence-specific sgRNA, with germline transmission established through backcrossing of founder animals.

**Table 1 Mice models with PMR KO were generated for the study.**

| Animal | Strain | Gene Target | Deletion Type | Reference |
|---|---|---|---|---|
| **Ninj1 Intestinal KO** | *Ninj1* $^{fl/fl}$ *Vil1*-Cre | NINJ1 exon 2 | Conditional | This study |
| **Ninj1 Intestinal KO** | *Ninj1* $^{fl/fl}$ *Vil1*-CreERT2 | NINJ1 exon 2 | Conditional | This study |
| **Ninj2 Intestinal KO** | *Ninj2* $^{fl/fl}$ *Vil1*-Cre | NINJ2 exon 2 | Conditional | This study |
| **Ninj1 Ninj2 Intestinal Double KO** | *Ninj1* $^{fl/fl}$ *Ninj2* $^{fl/fl}$ *Vil1*-Cre | NINJ1 exon 2<br>NINJ2 exon 2 | Conditional | This study |
| **Ninj1 Systematic KO** | *Ninj1* $^{fl/fl}$ CreERT2 | NINJ1 exon 2 | Inducible<br>Conditional | This study |
| **Ninj2 Systemic KO** | *Ninj2* $^{-/-}$ | NINJ2 exon 2 | Conventional | This study |
| **GsdmD GsdmE Systemic Double KO** | *GsdmD* $^{-/-}$ *GsdmE* $^{-/-}$ | GSDMD and GSDME | Conventional | The Jackson Lab |

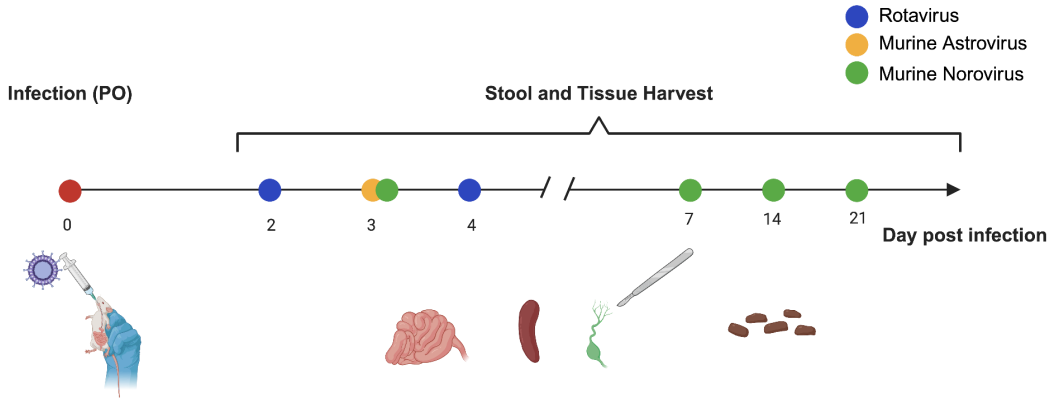


**Figure 3. Schematics for gut pathogen infection**

Adult mice from each genotype were infected with one of three gut-tropic viruses by oral gavage and monitored over the indicated time course. The red dot at day 0 indicates the point of inoculation. Colored dots indicate fecal and tissue collection timepoints for each virus: rotavirus (blue, days 2 and 4), murine astrovirus (MAstV, yellow, day 3), and murine norovirus (MNoV, green, days 3, 7, 14, and 21). Icons below the timeline indicate the biological samples collected at the indicated timepoints, including intestinal tissue, spleen, mesenteric lymph nodes, and fecal pellets. Viral burden was quantified from fecal pellets by qRT-PCR and expressed as genome copies per fecal pellet.

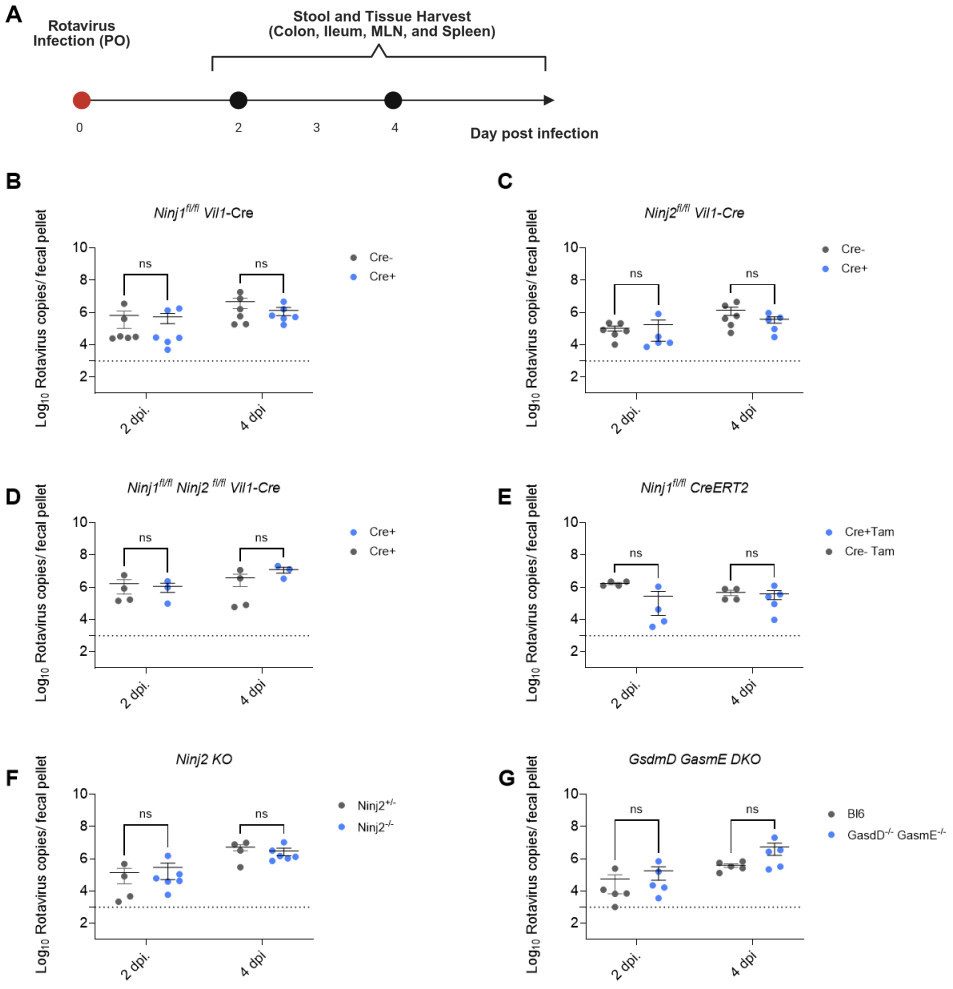


**Figure 4. Host genotype does not significantly alter rotavirus replication in the mouse gut.** A) Schematics of rotavirus infection timeline. Stool samples from B) *Ninj1*$^{fl/fl}$ Vil1-Cre, C) *Ninj2*$^{fl/fl}$ *Vil1*-Cre, D) *Ninj1*$^{fl/fl}$ *Ninj2*$^{fl/fl}$ *Vil1*-Cre, E) *Ninj1*$^{fl/fl}$ CreERT2, F) *Ninj2-/-* , and G) *GsdmD-/- GsdmE-/-* mice were analyzed at two timepoints. Blue dots represent the experimental animals while the grey dots represent the control animals. Viral burden was quantified by qRT-PCR and expressed as genome copies per sample. Data are pooled from five independent experiments with more than 2 mice per genotype per experiment. The limit of detection is $10^3$ genome copies. Statistical analyses were performed using the multiple Mann–Whitney test with p value less than 0.05 considered as significant. NS, not significant.

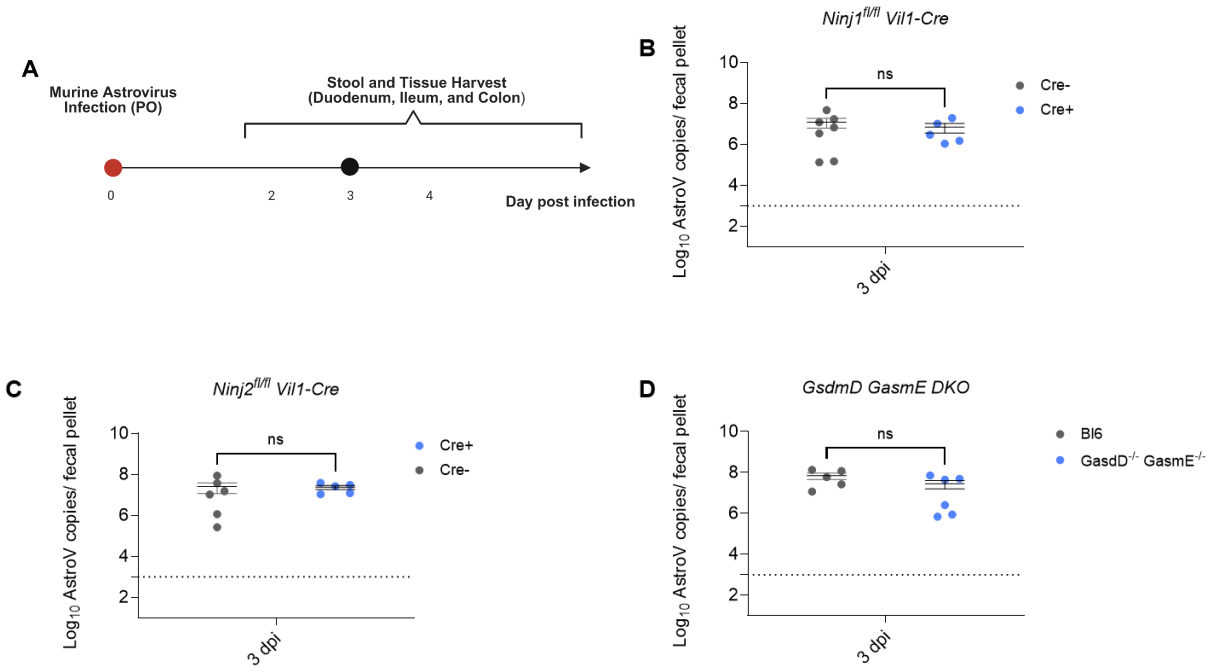


**Figure 5. Astrovirus replication in the mouse gut is not significantly affected by host genotype.**

A) Schematics of murine astrovirus infection timeline. Stool samples from B) *Ninj1*$^{fl/fl}$ Vil1-Cre, C) *Ninj2*$^{fl/fl}$ *Vil1*-Cre, D) *GsdmD-/- GsdmE-/-* mice were analyzed. Blue dots represent the experimental animals while the grey dots represent the control animals. Viral burden was quantified by qRT-PCR and expressed as genome copies per sample. Data are pooled from five independent experiments with more than 2 mice per genotype per experiment. The limit of detection is $10^3$ genome copies. Statistical analyses were performed using the multiple Mann–Whitney test with p value less than 0.05 considered as significant. NS, not significant.

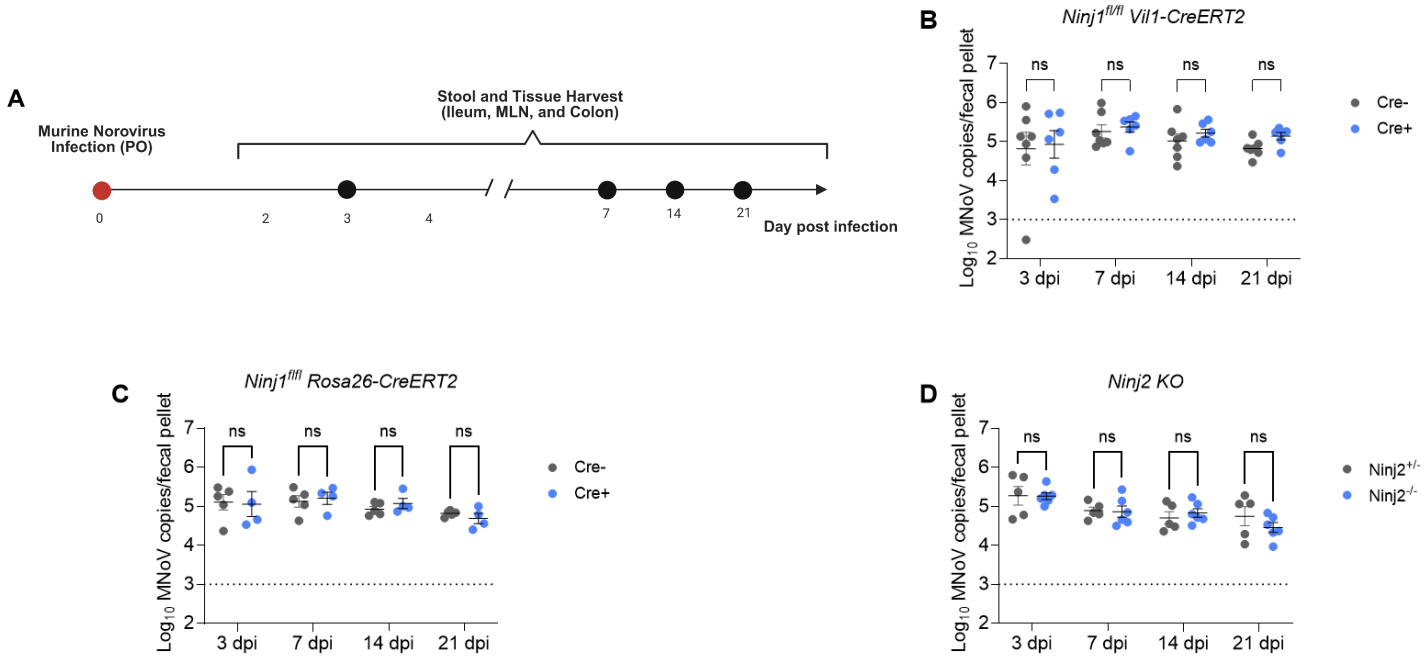


**Figure 6. Murine Norovirus replication is not significantly impacted by PMR genotype**
A) Schematics of murine norovirus infection timeline. Stool samples from B) *Ninj1*$^{fl/fl}$ Vil1-CreERT2, C) *Ninj1*$^{fl/fl}$ *Rosa26*-CreERT2, D) *Ninj2-/-* mice were analyzed. Blue dots represent the experimental animals while the grey dots represent the control animals. Viral burden was quantified by qRT-PCR and expressed as genome copies per sample. Data are pooled from five independent experiments with more than 2 mice per genotype per experiment. The limit of detection is $10^3$ genome copies. Statistical analyses were performed using the multiple Mann–Whitney test with p value less than 0.05 considered as significant. NS, not significant.

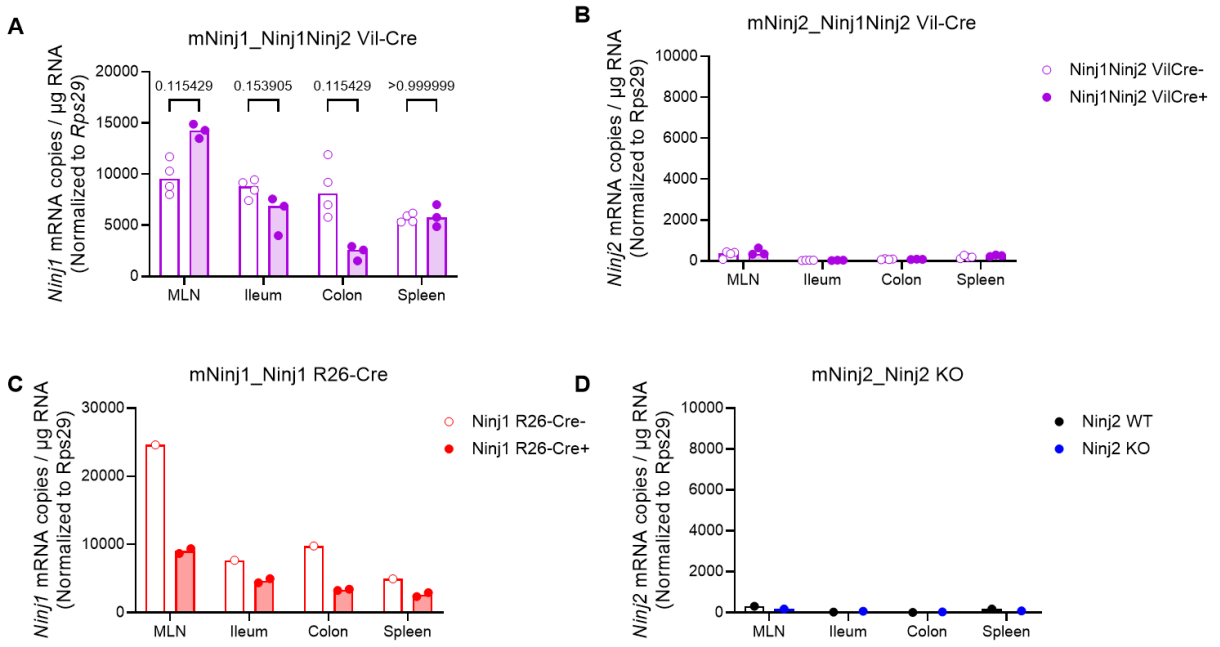


**Figure 7 NINJ1 and NINJ2 mRNA levels in mice tissue samples**

Tissue samples from A, B) Ninj1$^{fl/fl}$ Ninj2$^{fl/fl}$ *Vil1*-Cre, C) Ninj1$^{fl/fl}$ *Rosa26*-CreERT, D) Ninj2-/- mice and control mice are analyzed for mRNA levels for *Ninj1* and *Ninj2* to confirm knockout. Empty dots represent control mice and filled dots represent knockout mice. Statistical analyses were performed using the multiple Mann–Whitney test with p value less than 0.05 considered as significant. NS, not significant.

## References


Angosto-Bazarra, D., Alarcón-Vila, C., Hurtado-Navarro, L., Baños, M. C., Rivers-Auty, J., & Pelegrín, P. (2022). Evolutionary analyses of the gasdermin family suggest conserved roles in infection response despite loss of pore-forming functionality. *BMC Biology*, *20*(1), 9. https://doi.org/10.1186/s12915-021-01220-z

Araki, T., & Milbrandt, J. (1996). Ninjurin, a Novel Adhesion Molecule, Is Induced by Nerve Injury and Promotes Axonal Growth. In *Neuron* (Vol. 17).

Araki, T., & Milbrandt, J. (1999). *Ninjurin2, a Novel Homophilic Adhesion Molecule, Is Expressed in Mature Sensory and Enteric Neurons and Promotes Neurite Outgrowth*.

Borges, J. P., Sætra, R. S., Volchuk, A., Bugge, M., Devant, P., Sporsheim, B., Kilburn, B. R., Evavold, C. L., Kagan, J. C., Goldenberg, N. M., Flo, T. H., & Steinberg, B. E. (2022). Glycine inhibits NINJ1 membrane clustering to suppress plasma membrane rupture in cell death. *eLife*, *11*. https://doi.org/10.7554/eLife.78609

David, L., Borges, J. P., Hollingsworth, L. R., Volchuk, A., Jansen, I., Garlick, E., Steinberg, B. E., & Wu, H. (2024). NINJ1 mediates plasma membrane rupture by cutting and releasing membrane disks. *Cell*, *187*(9), 2224-2235.e16. https://doi.org/10.1016/j.cell.2024.03.008

Degen, M., Santos, J. C., Pluhackova, K., Cebrero, G., Ramos, S., Jankevicius, G., Hartenian, E., Guillerm, U., Mari, S. A., Kohl, B., Müller, D. J., Schanda, P., Maier, T., Perez, C., Sieben, C., Broz, P., & Hiller, S. (2023). Structural basis of NINJ1-mediated plasma membrane rupture in cell death. *Nature*, *618*(7967), 1065–1071. https://doi.org/10.1038/s41586-023-05991-z

Dickson, I. (2017). Inflammasome modulates rotavirus infection. *Nature Reviews Gastroenterology & Hepatology*, *14*(8), 450–450. https://doi.org/10.1038/nrgastro.2017.94

Dondelinger, Y., Priem, D., Huyghe, J., Delanghe, T., Vandenabeele, P., & Bertrand, M. J. M. (2023). NINJ1 is activated by cell swelling to regulate plasma membrane permeabilization during regulated necrosis. *Cell Death and Disease*, *14*(11). https://doi.org/10.1038/s41419-023-06284-z

Evavold, C. L., Ruan, J., Tan, Y., Xia, S., Wu, H., & Kagan, J. C. (2018). The

Pore-Forming Protein Gasdermin D Regulates Interleukin-1 Secretion from Living Macrophages. *Immunity*, *48*(1), 35-44.e6. https://doi.org/10.1016/j.immuni.2017.11.013

Hall, A. J., Glass, R. I., & Parashar, U. D. (2016). New insights into the global burden of noroviruses and opportunities for prevention. In *Expert Review of Vaccines* (Vol. 15, Issue 8, pp. 949–951). Taylor and Francis Ltd. https://doi.org/10.1080/14760584.2016.1178069

Hartenian, E., Agustoni, M., & Broz, P. (2026). NINJ1 blocks HSV-1 entry into macrophages to impact viral replication and immunity. *EMBO Reports*, *27*(1), 69–88. https://doi.org/10.1038/s44319-025-00638-8

Imre, G. (2020). Cell death signalling in virus infection. In *Cellular Signalling* (Vol. 76). Elsevier Inc. https://doi.org/10.1016/j.cellsig.2020.109772

Ingle, H., Hassan, E., Gawron, J., Mihi, B., Li, Y., Kennedy, E. A., Kalugotla, G., Makimaa, H., Lee, S., Desai, P., McDonald, K. G., Diamond, M. S., Newberry, R. D., Good, M., & Baldridge, M. T. (2021). Murine astrovirus tropism for goblet cells and enterocytes facilitates an IFN-λ response in vivo and in enteroid cultures. *Mucosal Immunology*, *14*(3), 751–761. https://doi.org/10.1038/s41385-021-00387-6

Kayagaki, N., Kornfeld, O. S., Lee, B. L., Stowe, I. B., O'Rourke, K., Li, Q., Sandoval, W., Yan, D., Kang, J., Xu, M., Zhang, J., Lee, W. P., McKenzie, B. S., Ulas, G., Payandeh, J., Roose-Girma, M., Modrusan, Z., Reja, R., Sagolla, M., … Dixit, V. M. (2021). NINJ1 mediates plasma membrane rupture during lytic cell death. *Nature*, *591*(7848), 131–136. https://doi.org/10.1038/s41586-021-03218-7

Kayagaki, N., Stowe, I. B., Lee, B. L., O'Rourke, K., Anderson, K., Warming, S., Cuellar, T., Haley, B., Roose-Girma, M., Phung, Q. T., Liu, P. S., Lill, J. R., Li, H., Wu, J., Kummerfeld, S., Zhang, J., Lee, W. P., Snipas, S. J., Salvesen, G. S., … Dixit, V. M. (2015). Caspase-11 cleaves gasdermin D for non-canonical inflammasome signalling. *Nature*, *526*(7575), 666–671. https://doi.org/10.1038/nature15541

Lee, S., Liu, H., Wilen, C. B., Sychev, Z. E., Desai, C., Hykes, B. L., Orchard, R. C., McCune, B. T., Kim, K. W., Nice, T. J., Handley, S. A., Baldridge, M. T., Amarasinghe, G. K., & Virgin, H. W. (2019). A Secreted Viral Nonstructural Protein Determines Intestinal Norovirus Pathogenesis. *Cell Host and Microbe*, *25*(6), 845-857.e5. https://doi.org/10.1016/j.chom.2019.04.005

Morita, H., Yasuda, M., Yamamoto, M., Tomiyama, Y., Uchida, R., Ka, Y., Ogura, T., Kawai, K., Suemizu, H., & Hayashimoto, N. (2021). Pathogenesis of murine astrovirus in experimentally infected mice. *Experimental Animals*, *70*(3), 355–363. https://doi.org/10.1538/expanim.20-0162

Nössing, C., & Ryan, K. M. (2023). 50 years on and still very much alive: 'Apoptosis: a basic biological phenomenon with wide-ranging implications in tissue kinetics.' *British Journal of Cancer*, *128*(3), 426–431. https://doi.org/10.1038/s41416-022-02020-0

Pawłuszkiewicz, K., Ryglowski, P. J., Idzik, N., Błaszczyszyn, K., Kucharczyk, E., Gaweł-Dąbrowska, D., Siczek, M., Widelski, J., & Paluch, E. (2025). Rotavirus Infections: Pathophysiology, Symptoms, and Vaccination. In *Pathogens* (Vol. 14, Issue 5). Multidisciplinary Digital Publishing Institute (MDPI). https://doi.org/10.3390/pathogens14050480

Sahoo, B., Mou, Z., Liu, W., Dubyak, G., & Dai, X. (2025). How NINJ1 mediates plasma membrane rupture and why NINJ2 cannot. *Cell*, *188*(2), 292-302.e11. https://doi.org/10.1016/j.cell.2024.11.021

Sborgi, L., Rühl, S., Mulvihill, E., Pipercevic, J., Heilig, R., Stahlberg, H., Farady, C. J., Müller, D. J., Broz, P., & Hiller, S. (2016). GSDMD membrane pore formation constitutes the mechanism of pyroptotic cell death. *The EMBO Journal*, *35*(16), 1766–1778. https://doi.org/10.15252/embj.201694696

Shen, S., Shao, Y., & Li, C. (2023). Different types of cell death and their shift in shaping disease. In *Cell Death Discovery* (Vol. 9, Issue 1). Springer Nature. https://doi.org/10.1038/s41420-023-01581-0

Shi, J., Zhao, Y., Wang, K., Shi, X., Wang, Y., Huang, H., Zhuang, Y., Cai, T., Wang, F., & Shao, F. (2015). Cleavage of GSDMD by inflammatory caspases determines pyroptotic cell death. *Nature*, *526*(7575), 660–665. https://doi.org/10.1038/nature15514

Song, J., Zhang, L., Moon, S., Fang, A., Wang, G., Gheshm, N., Loeb, S. A., Cao, P., Wallace, J. R., Alfajaro, M. M., Strine, M. S., Beatty, W. L., Jamieson, A. M., Orchard, R. C., Robinson, B. A., Nice, T. J., Wilen, C. B., Orvedahl, A., Reese, T. A., & Lee, S. (2025). Norovirus co-opts NINJ1 for selective protein secretion. *Science Advances*, *11*(9). https://doi.org/10.1126/sciadv.adu7985

Wang, C., Dreyer, B., Teran, E., & Ruan, J. (2025). From pores to rupture: Structural

basis and regulation of lytic cell death by gasdermins and NINJ1. In *Journal of Biological Chemistry* (Vol. 301, Issue 10). American Society for Biochemistry and Molecular Biology Inc. https://doi.org/10.1016/j.jbc.2025.110698

Wang, Y., Gao, W., Shi, X., Ding, J., Liu, W., He, H., Wang, K., & Shao, F. (2017). Chemotherapy drugs induce pyroptosis through caspase-3 cleavage of a gasdermin. *Nature*, *547*(7661), 99–103. https://doi.org/10.1038/nature22393

Zhang, J., Bustamante, M., Shi, Y., Nakajima, K., & Chen, X. (2026). *Nerve Injury-Induced Protein 2 preserves lysosomal membrane integrity to suppress ferroptosis*. https://doi.org/10.64898/2026.02.09.704867

Zhang, J., Kong, X., Yang, H. J., Zhang, W., Chen, M., & Chen, X. (2024). Ninjurin 2 Modulates Tumorigenesis, Inflammation, and Metabolism via Pyroptosis. *American Journal of Pathology*, *194*(5), 849–860. https://doi.org/10.1016/j.ajpath.2024.01.013